

Heavy-Quark Spectra at RHIC and Resonances in the QGP

R. Rapp^a, V. G. Koch^b and H. van Hees^a

^aCyclotron Institute and Physics Department, Texas A & M University, College Station, Texas 77843-3366, USA

^bLaboratori Nazionali del Sud INFN, via S. Sofia 62, I-95123 Catania, Italy

Thermalization and collective flow of charm (c) and bottom (b) quarks are evaluated from elastic parton scattering via \bar{D} and \bar{B} meson resonances in an expanding, strongly interacting quark-gluon plasma at RHIC. Pertinent drag and diffusion coefficients are implemented into a relativistic Langevin simulation to compute transverse momentum spectra and azimuthal flow asymmetries (v_2) of c - and b -quarks. Upon hadronization (including coalescence and fragmentation) and semileptonic D - and B -decays, the resulting electron spectra (R_{AA} and v_2) are compared to recent RHIC data.

1. Introduction

Among the key challenges in describing the hot and dense matter created in Au-Au collisions at the Relativistic Heavy-Ion Collider (RHIC) is the understanding of the microscopic interactions providing a rapid thermalization as inferred from hydrodynamic models. Heavy quarks are valuable probes in this respect as they are produced early in the collision and thus sense the subsequent evolution down to rather soft momenta.

First data on single-electron (e^-) spectra, associated with semileptonic decays of D and B -mesons, have revealed a surprisingly large suppression (small R_{AA}^e) and azimuthal asymmetry (v_2^e) [1, 2, 3]. On the one hand, within quark coalescence models [4, 5, 6] of a hadronizing quark plasma, the v_2^e data favor the assumption that charm quarks exhibit a degree of thermalization comparable to that of light partons [4]. On the other hand, within radiative energy-loss calculations in a gluon plasma [7, 8], the R_{AA}^e data require significantly larger transport coefficients than expected within perturbative Quantum Chromodynamics (pQCD). While for lower p_T energy loss due to elastic scattering becomes parametrically dominant (by $1 = \frac{p_T}{s}$) [9], elastic pQCD cross sections [10, 11] with realistic values for the strong coupling constant ($\alpha_s = 0.3-0.5$) cannot account for the observed effects either [9, 12]. In addition, the contribution of B -meson decays is expected to further reduce both suppression and elliptic flow signals in the electron spectra.

In this talk we address the question of the microscopic interactions in a strongly interacting Quark-Gluon Plasma (QGP) by introducing D - and B -meson states providing for elastic resonance cross sections for c - and b -quarks [13]. Corresponding drag and diffusion coefficients are implemented into a relativistic Langevin simulation for semi-central Au-Au collisions at RHIC, with subsequent comparisons to single- e^- observables [12].

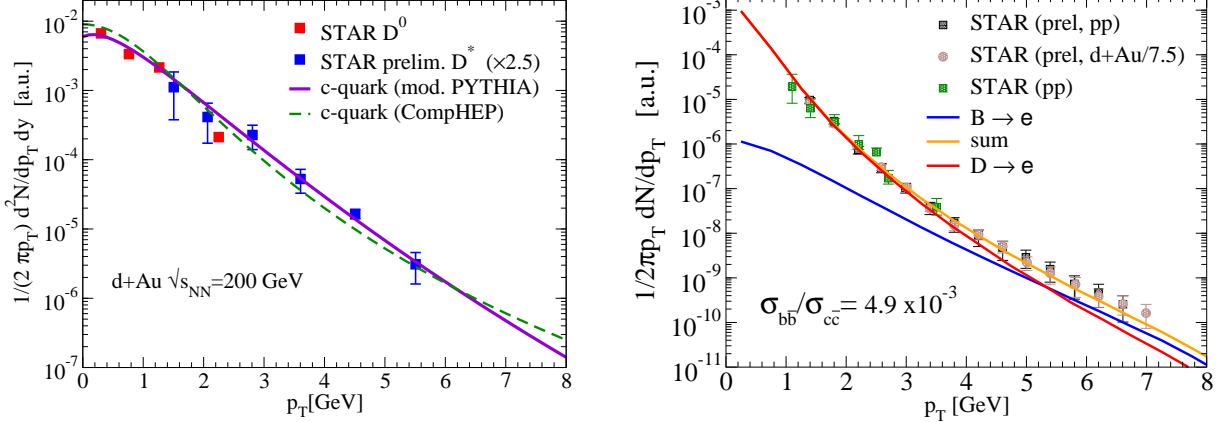


Figure 1. Our fit of initial c- and b-quark spectra using experimental spectra for D - and D^* -mesons [14, 15] (left panel) and single e^- [16, 15] (right panel).

2. Heavy-Quark Scattering in the QGP

Lattice QCD computations of hadronic correlators suggest the survival of mesonic resonance/bound states up to temperatures of $2T_c$ in both heavy- and light-quark sectors [17, 18], cf. also Refs. [19, 20, 21]. Here, we simply assume the existence of the lowest-lying, pseudoscalar D (B) meson as a resonance 0.5 GeV above the heavy-light quark threshold [13]. The pertinent effective Lagrangian with chiral and heavy-quark (HQ) symmetry then dictates the degeneracy of the $J^P = 0^-$ state with vector, scalar and axial-vector partners. The 2 free parameters are the resonance masses ($m_{D(B)} = 2(5)$ GeV, with $m_{c(b)} = 1.5(4.5)$ GeV) and widths (varied as $= 0.4-0.75$ GeV). For strange quarks we only include pseudoscalar and vector states. The resonant $Q\bar{q}$ cross sections are supplemented with leading-order pQCD scattering of partons [22] dominated by t-channel gluon exchange and regularized by a Debye mass $m_g = gT$ with $s = g^2/(4\pi) = 0.4$. When evaluating drag and diffusion coefficients in a Fokker-Planck approach [10], the resonances reduce HQ thermalization times by a factor of 3 below pQCD scattering [13].

The heavy quarks are implemented into $b=7$ fm $Au-Au$ collisions at RHIC via relativistic Langevin simulations [9] in an isentropically expanding isotropic QGP reball. The expansion parameters are fixed to closely resemble the time evolution of radial and elliptic flow in hydrodynamic models [23], with an appropriate hadron multiplicity at chemical freezeout. A formation time of $1/3$ fm/c translates into an initial temperature of $T_0 = 340$ MeV, based on an ideal QGP equation of state with 2.5 avors. The Langevin process is simulated in the H anggi-K limontovich realization [24], i.e., in the local rest frame of the bulk matter with an update of HQ position and momentum given by

$$\dot{x} = \frac{p}{E} \quad t; \quad \dot{p} = -A(t; p + \dot{p})p - t + \dot{W}(t; p + \dot{p}) \quad (1)$$

(E : HQ energy); \dot{W} is a random force distributed according to Gaussian noise,

$$h \quad i$$

 $P(W) / \exp \hat{B}_{jk} W^j W^k = (4\pi t)^{-3/2} \quad (2)$

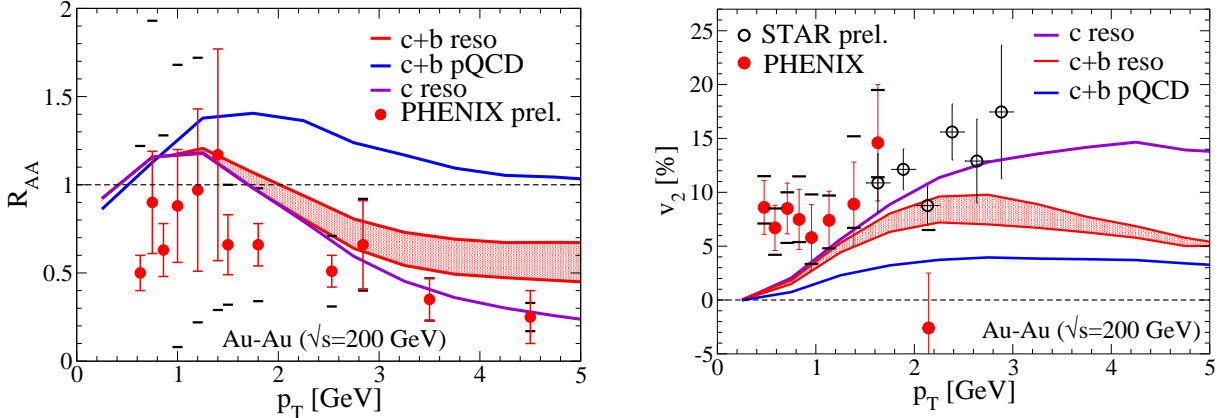


Figure 2. Nuclear modification factor (R_{AA} , left panel) and elliptic flow (v_2 , right panel) of semi-leptonic D- and B-meson decay electrons in $b=7$ fm $\sqrt{s_{NN}} = 200$ GeV Au-Au collisions assuming di erent elastic heavy-quark interactions in the QGP with subsequent coalescence+fragmentation hadronization, compared to PHENIX and STAR data [1, 2, 3].

The drag coe cient (inverse relaxation time), A , and the di usion-coe cient matrix,

$$B_{jk} = (\hat{B}^{-1})_{jk} = B_0 (\delta^{jk} - \hat{p}^j \hat{p}^k) + B_1 \hat{p}^j \hat{p}^k; \quad (3)$$

follow from the microscopic model sketched above [13]. The thermal equilibrium limit is enforced by setting the longitudinal di usion coe cient to $B_1 = T E A$ [9]. HQ momenta are Lorentz-boosted to the laboratory frame according to the local bulk matter velocity.

To determine the initial HQ transverse-momentum (p_T) distributions and the relative magnitude of the c- and b-quark spectra, we use a modified PYTHIA c-quark spectrum and -function fragmentation to STAR D and D* spectra in d-Au collisions [14, 15] (left panel of Fig. 1). The pertinent e -decay spectra saturate data from p-p and d-Au up to $p_T' = 3.5$ GeV [16, 15] (right panel of Fig. 1). The missing yield at higher p_T is then attributed to B-meson decays, resulting in a cross section ratio of $\eta_{bb} = \eta_{cc} = 4.9 \cdot 10^3$ and implying a crossing of D- and B -decay electrons at $p_T' = 5$ GeV.

3. Hadronization and Single-Electron Spectra

To compare our results for the final HQ p_T -spectra and v_2 , recorded at the end of the mixed phase, to measured e -spectra in Au-Au collisions, we hadronize b- and c-quarks using the coalescence model of Ref. [4] based on Ref. [25] for the light-quark distributions. While this essentially exhausts the HQ yields at low p_T , the decreasing light-quark phase-space density at higher p_T implies unpaired c- and b-quarks which we hadronize via -function fragmentation. The single-e -spectra follow from D- and B-meson 3-body decays, cf. Fig. 2. Compared to elastic pQCD rescattering alone, resonance effects manifest themselves as a substantial increase (decrease) in v_2^e (R_{AA}^e), while coalescence further amplifies v_2^e but also increases R_{AA}^e . The bottom contributions reduce the effects starting from electron momenta of about 3 GeV. Overall, the main trends in the data are reasonably well reproduced.

4. Conclusions

Based on elastic resonant interactions in the sQGP we have evaluated c- and b-spectra in an expanding fireball at RHIC employing relativistic Langevin simulations. The much increased cross sections compared to pQCD lead to c-quark R_{AA} and v_2 of down to 0.2 and up to 10%, respectively, while b-quarks are less affected. After subsequent hadronization in a combined quark-coalescence and fragmentation scheme followed by semi-leptonic decays, we have found that resonant interactions may play an important role in the simultaneous understanding of the nuclear modification factor and elliptic flow of heavy-quark observables (including single electrons) at RHIC, and thus open a promising window on the microscopic properties of the sQGP including its rapid thermalization behavior.

Acknowledgments. This work has been supported in part by a U.S. National Science Foundation CAREER award under grant PHY-0449489.

REFERENCES

1. S.S. Adler et al. [PHENIX Collaboration], Phys. Rev. C 72, 024901 (2005).
2. F. Laue et al. [STAR Collaboration], J. Phys. G 31, S27 (2005).
3. B. Jacak et al. [PHENIX Collaboration], to appear in Proc. of 5th International Conference on Physics and Astrophysics of Quark Gluon Plasma (2005), nucl-ex/0508036.
4. V. G reco, C.M. Ko and R. Rapp, Phys. Lett. B 595, 202 (2004).
5. D. Molnar, J. Phys. G 31, S421 (2005).
6. B. Zhang, L.W. Chen and C.M. Ko, Phys. Rev. C 72, 024906 (2005).
7. M. Djordjevic, M. Gyulassy and S. Wicks, Phys. Rev. Lett. 94, 112301 (2005).
8. N. Armesto et al., Phys. Rev. D 71, 054027 (2005).
9. G.D. Moore and D. Teaney, Phys. Rev. D 71, 064904 (2005).
10. B. Svetitsky, Phys. Rev. D 37, 2484 (1988).
11. M. G. Mustafa and M. H. Thomas, Acta Phys. Hung. A 22, 93 (2005).
12. H. van Hees, V. G reco and R. Rapp (2005), nucl-th/0508055.
13. H. van Hees and R. Rapp, Phys. Rev. C 71, 034907 (2005).
14. J. Adams et al. [STAR Collaboration], Phys. Rev. Lett. 94, 062301 (2005).
15. A. Tai et al. [STAR Collaboration], J. Phys. G 30, S809 (2004).
16. A.A.P. Suaide et al. [STAR Collaboration], J. Phys. G 30, S1179 (2004).
17. M. Asakawa and T. Hatsuwa, Phys. Rev. Lett. 92, 012001 (2004).
18. F. Karsch and E. Laermann, hep-lat/0305025.
19. E.V. Shuryak and I. Zahed, Phys. Rev. C 70, 021901(R) (2004).
20. C.Y. Wong (2004), hep-ph/0408020.
21. M. Mannarelli and R. Rapp (2005), hep-ph/0505080.
22. B.L. Combridge, Nucl. Phys. B 151, 429 (1979).
23. P.F. Kolb, J. Sollfrank and U. Heinz, Phys. Rev. C 62, 054909 (2000).
24. J. Dunkel and P. Haggi, Phys. Rev. E 71, 016124 (2005).
25. V. G reco, C.M. Ko and P. Levai, Phys. Rev. C 68, 034904 (2003).